



Synthesis and molecular docking of new *N*-4-piperazinyl ciprofloxacin hybrids as antimicrobial DNA gyrase inhibitors

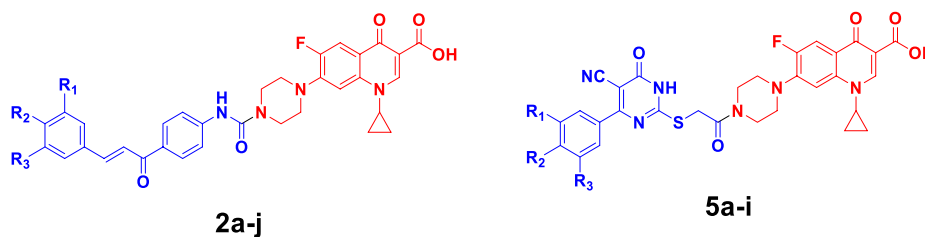
Hamada H. H. Mohammed^{1,2,3} · Doaa Mohamed Elroby Ali⁴ · Mohamed Badr⁵ · Ahmed G. K. Habib⁶ · Abobakr Mohamed Mahmoud⁷ · Sarah M. Farhan⁷ · Shima Salah Hassan Abd El Gany⁷ · Soad A. Mohamad⁸ · Alaa M. Hayallah^{9,10} · Samar H. Abbas² · Gamal El-Din A. Abuo-Rahma^{2,3}

Received: 26 May 2022 / Accepted: 11 September 2022 / Published online: 24 September 2022
© The Author(s) 2022

Abstract

A series of *N*-4 piperazinyl ciprofloxacin derivatives as urea-tethered ciprofloxacin-chalcone hybrids **2a-j** and thioacetyl-linked ciprofloxacin-pyrimidine hybrids **5a-i** were synthesized. The target compounds were investigated for their antibacterial activity against *S. aureus*, *P. aeruginosa*, *E. coli*, and *C. albicans* strains, respectively. Ciprofloxacin derivatives **2a-j** and **5a-i** revealed broad antibacterial activity against either Gram positive or Gram negative strains, with MIC range of 0.06–42.23 µg/mL compared to ciprofloxacin with an MIC range of 0.15–3.25 µg/mL. Among the tested compounds, hybrids **2b**, **2c**, **5a**, **5b**, **5h**, and **5i** exhibited remarkable antibacterial activity with MIC range of 0.06–1.53 µg/mL against the tested bacterial strains. On the other hand, compounds **2c**, **2e**, **5c**, and **5e** showed comparable antifungal activity to ketoconazole against *candida albicans* with MIC range of 2.03–3.89 µg/mL and 2.6 µg/mL, respectively. Further investigations showed that some ciprofloxacin hybrids have inhibitory activity against DNA gyrase as potential molecular target compared to ciprofloxacin with IC₅₀ range of 0.231 ± 0.01–7.592 ± 0.40 µM and 0.323 ± 0.02 µM, respectively. Docking studies of compounds **2b**, **2c**, **5b**, **5c**, **5e**, **5h**, and **5i** on the active site of DNA gyrase (PDB: 2XCT) confirmed their ability to form stable complex with the target enzyme like that of ciprofloxacin.

Graphical abstract



Compound	MIC (µg/mL)				IC ₅₀ ±SD (µM)
	Gram-positive	Gram-negative		Fungi	<i>S. aureus</i> DNA gyrase
	<i>S. aureus</i>	<i>E. coli</i>	<i>P. aeruginosa</i>	<i>C. albicans</i>	
2a-j	0.06-8.00	0.18-16.98	0.64-6.25	15.23	0.231±0.01-3.81±0.20
5a-i	0.28-8.14	0.12-42.23	1.03	0.12-23.12	1.012±0.05-4.546±0.24
Ciprofloxacin	3.25	0.15	0.22	>100	0.323±0.02
ketoconazole	--	--	--	2.6	-----

Keywords Ciprofloxacin chalcone · Ciprofloxacin pyrimidine · DNA gyrase inhibitors · Antimicrobial

Extended author information available on the last page of the article

Introduction

The prevalence of bacterial resistance to therapeutically used antibiotics is a global health problem that encouraged scientists to develop new antibiotics [1, 2]. Therefore, novel antibacterial agents that have little or no bacterial resistance are urgently required to improve the efficiency of antibiotics against microbes [3]. One of the important strategies to do this is modifying the structural features of the existing antibiotics [4, 5]. In this situation, the development of antibiotic hybrids can function properly because it requires no validation of novel biological targets or the discovery of new antibacterial pharmacophores [6]. This strategy involves linking two or more antibiotics that inhibit different targets in bacteria into one single molecule [7, 8]. It is believed that hybrid molecules act by inhibiting two or multi targets simultaneously, increasing potency against drug-resistant bacterial strains, expanding the spectrum of activity, and decreasing the possibility of developing bacterial resistance [6, 9]. Ciprofloxacin is a broad-spectrum antibacterial agent with an excellent safety profile [10]. It is widely used for the treatment of bacterial infection, and as a second-line agent for management of tuberculosis (TB) [11]. It achieves its antibacterial effect by inhibiting bacterial DNA gyrase (topoisomerase II) which involved in DNA replication [10, 12]. It was reported that position 7 in quinolones and fluoroquinolones is responsible for interaction with DNA gyrase, or topoisomerase IV [13–15]. The nature of the substituent at position 7 greatly influences spectrum, potency, and

pharmacokinetics [16, 17]. The introduction of a bulky substituent at position 7 was found to diminish the likelihood of bacterial resistance in wild-type bacterial strains and improved potency against anaerobic bacteria [9–11]. Recent research studies revealed that substituting the *N*-4 piperazine heterocycle of ciprofloxacin with a lipophilic substituent was found to enhance its antibacterial and antimycobacterial activities [16, 17]. Also, It was reported that 1,2,4-triazole-5(4*H*)-thione ciprofloxacin hybrid **I** revealed remarkable in vitro antibacterial activity against all tested strains, either Gram-positive or Gram-negative pathogens with MIC < 0.24 µg/mL and 0.01 to 1.32 µg/mL, respectively, compared to ampicillin (MIC: 3.9–250 µg/mL) (Fig. 1) [18, 19]. The oxazolidinone-ciprofloxacin hybrid **II** displayed potent in vitro activity against Gram negative and Gram positive with MIC range 0.125–4 µg/mL and remarkable potency against fluoroquinolones, vancomycin, and/or linezolid-resistant strains with MIC range 0.25–0.5 µg/mL (Fig. 1) [20]. On the other hand, Chalcones, known as α,β -unsaturated ketones, are essential building pharmacophores in many drug design protocols [21]. Chalcone-containing compounds are of special interest because of the ease of their synthesis, improved lipophilic profile, and pronounced antimicrobial activities [21–23]. They showed broad spectrum of pharmacological activities such as antibacterial [24], antimalarial [25], antifungal [26], antiviral [27], anti-inflammatory [28], and anticancer activities [29, 30]. Another moiety of high importance in medicinal chemistry is the pyrimidine core [31]. Pyrimidine-containing compounds have been well recognized for their versatile therapeutic applications such

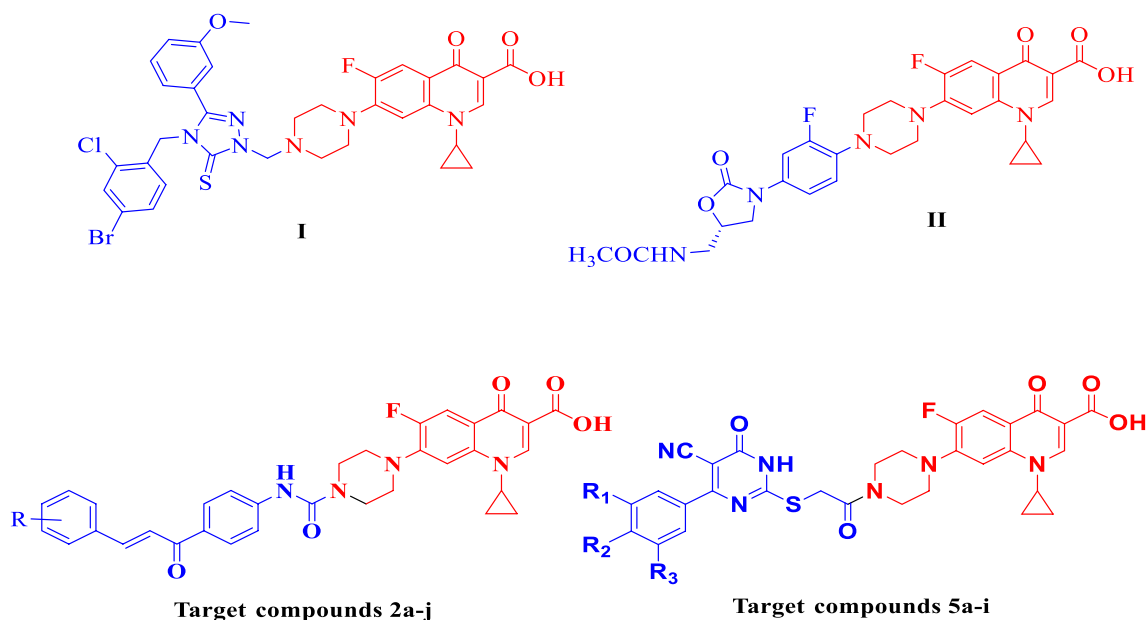
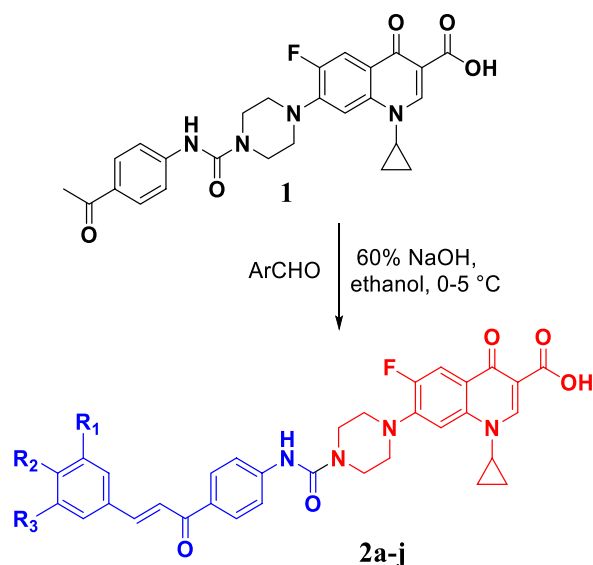


Fig. 1 Structures of some reported ciprofloxacin derivatives and target compounds **2a-j** and **5a-i**

Scheme 1 Synthesis of target ciprofloxacin hybrids 2a–j

- 2a:** $R_1=R_2=R_3=H$
2b: $R_1=Cl; R_2=R_3=H$
2c: $R_1=R_3=H; R_2=Cl$
2d: $R_1=R_3=H; R_2=Br$
2e: $R_1=R_3=H; R_2=F$
2f: $R_1=R_3=H; R_2=Me$
2g: $R_1=R_3=H; R_2=OMe$
2h: $R_1=R_3=H; R_2=N(Me)_2$
2i: $R_1=R_2=OMe; R_3=H$
2j: $R_1=R_2=R_3=OMe$



as anticancer [32], antimalarial [33], antiviral [34], antibacterial [35, 36], antifungal [37, 38], and anticonvulsant [39]. Based on molecular hybridization, linking of ciprofloxacin at its *N*-4 piperazine moiety with different biologically active scaffolds could result in hybrid molecules that could modulate more than one target, simultaneously enhancing its antibacterial activity.

Considering these issues, and due to the global health concern of bacterial resistance, this work aims to synthesize new ciprofloxacin-chalcone hybrids **2a-j** and new ciprofloxacin-pyrimidine hybrids **5a-j** and evaluation of their antibacterial and antifungal activities. Also, DNA gyrase assay was done as a potential target for the newly synthesized ciprofloxacin hybrids. Moreover, molecular docking studies were carried out to explore their binding modes.

Results and discussion

Chemistry

The *N*-4-piperazinyl ciprofloxacin-chalcones **2a-j** were prepared as reported by Condensation of compound **1** with various aromatic aldehydes in ethanol using 60% solution of sodium hydroxide to afford the target hybrids 2a-j in a good yield, Scheme 1 [30].

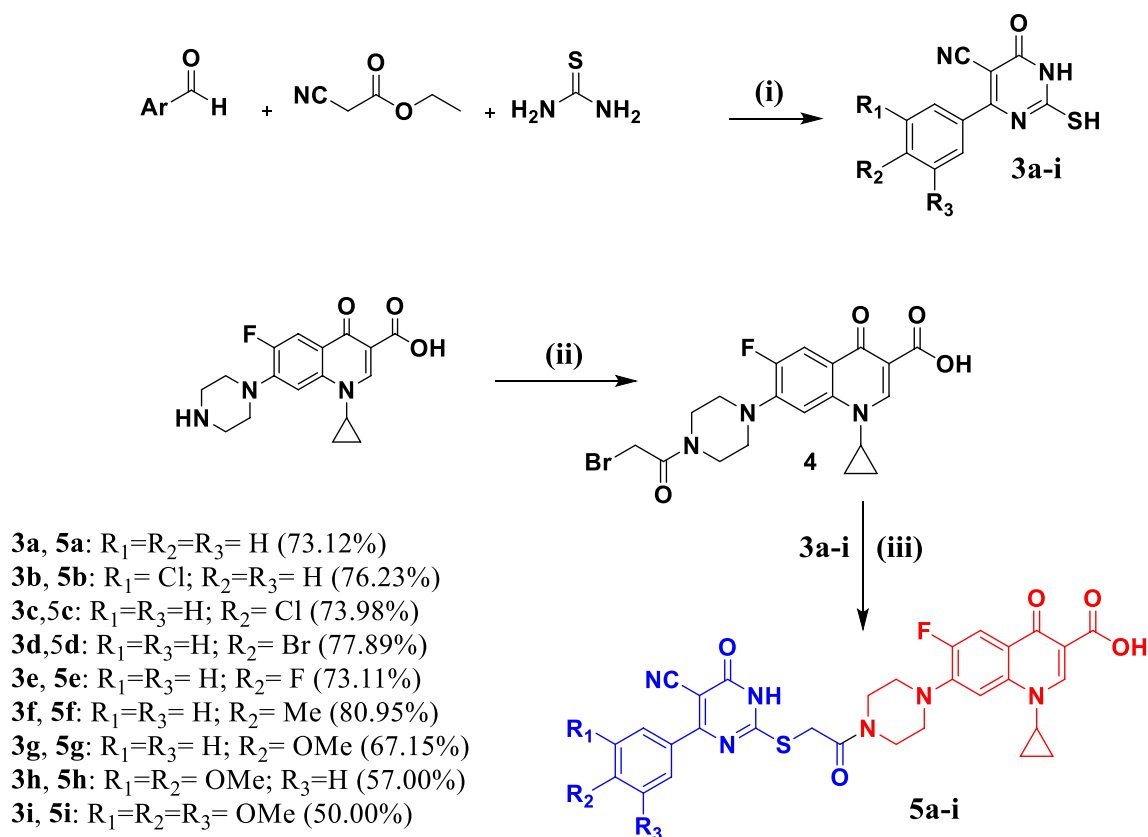
Reagents and conditions: (i) Appropriate aromatic aldehydes, 60% NaOH, ethanol, 0–5 °C stirring overnight, then neutralized with dil. acetic acid.

Moreover, the newly prepared ciprofloxacin-pyrimidine 5a-i were prepared as outlined in Scheme 2.

Reagent s and conditions: (i) Potassium carbonate, ethanol, reflux 8 h; (ii) Bromoacetyl bromide, triethylamine (TEA), dichloromethane, 0–5° C stirring overnight; (iii)

pyrimidine intermediate 5a-i, acetonitrile, triethylamine, reflux 4–6 h.

The desired intermediate pyrimidine derivatives **3a-i** were prepared as reported by heating at reflux a mixture of ethyl cyanoacetate, thiourea, and the appropriate aromatic aldehyde in absolute ethanol in the presence of potassium carbonate as a base [40, 41]. Ciprofloxacin derivative **4** was prepared by treating ciprofloxacin with bromoacetyl bromide in dichloromethane at 0 °C in the presence of TEA [42]. Alkylation of pyrimidine derivatives **3a-i** with compound **4** were achieved in acetonitrile in the presence of TEA according to a reported procedure [43, 44] to afford the target new compounds **5a-i**. The ¹H NMR spectra of compounds **5a-i** displayed the characteristic known pattern of fluoroquinolone scaffold. In addition, two doublets at $\delta = 7.53$ – 8.67 ppm indicated the presence of *para* disubstituted phenyl ring in their structures as in pyrimidine derivative **5f**. Moreover, compound **5e** showed triplet at $\delta = 7.38$ ppm of (*2H*) Ar–*H* due to fluorine coupling. Meanwhile, compound **5f** displayed singlet at $\delta = 2.30$ ppm corresponding Ar–*CH*₃. Likewise, the pyrimidine derivative **5g** revealed a singlet at $\delta = 3.84$ ppm belonging to the *p*-OCH₃ group. Also, **5h** displayed two singlets corresponding the presence of to the two methoxy groups at $\delta = 3.77$ and 3.84 ppm groups. Furthermore, **5i** showed two singlets for the three methoxy groups at $\delta = 3.78$ and 3.85 ppm and a singlet at $\delta = 7.36$ ppm which indicates the presence of 3,4,5-trimethoxyphenyl moiety. ¹³C NMR spectra of compounds **5a-i** revealed the characteristic pattern for fluoroquinolone nucleus and the carbonyl carbon of the thioacetyl linker, carbonyl of the carboxylic group, and C-6 of the dihydropyridine moiety, respectively. Also, ¹³C NMR spectra of compounds **5a-i** showed a characteristic signal at $\delta = 91.69$ – 93.06 ppm corresponding to the carbonitrile



Scheme 2 Synthesis of target compounds 5a–i

group. Data from the elemental analysis further confirmed the structures of the target compounds. Finally, Mass data for compounds **5a–i** confirmed their assigned structures. The m/z value of molecular ion peak $[M-H]^-$ for each compound was close to the calculated.

Biological Investigation

Screening of antibacterial and antifungal activities

The antibacterial and antifungal activities of compounds, ketone **1**, **2a–j**, and **5a–i** were evaluated in vitro against *S. aureus* (ATCC 6538), *P. aeruginosa* (ATCC 10,145), *E. coli* (ATCC 8739), and *C. albicans* (ATCC 10,231). Hybrids **2a–j** and the newly synthesized ciprofloxacin hybrids **5a–i** were evaluated against ciprofloxacin and ketoconazole as antibacterial and antifungal references, respectively using standard agar cup diffusion method [45]. Screening results are listed in Table 1. According to the results recorded in Table 1, it was found that hybrid **1** has a potent antibacterial activity against *S. aureus* compared to ciprofloxacin with MICs of 0.7 $\mu\text{g/mL}$ and 3.25 $\mu\text{g/mL}$, respectively. Also, it showed considerable activity against both of *E. coli* and *P. aeruginosa* compared to ciprofloxacin with MICs

of 0.60 $\mu\text{g/mL}$, 1.20 $\mu\text{g/mL}$, 0.15 $\mu\text{g/mL}$, and 0.22 $\mu\text{g/mL}$, respectively. Regarding the antibacterial activities of ciprofloxacin hybrids **2a–j**, compounds **2a**, **2b**, **2c**, **2e**, **2f**, and **2j** exhibited potent antibacterial activities against *S. aureus* compared to ciprofloxacin with MICs of 0.74 $\mu\text{g/mL}$, 0.06 $\mu\text{g/mL}$, 0.67 $\mu\text{g/mL}$, 0.89 $\mu\text{g/mL}$, 0.94 $\mu\text{g/mL}$, 1.48 $\mu\text{g/mL}$, and 3.25 $\mu\text{g/mL}$, respectively, while hybrids **2a**, **2b**, **2c**, and **2e** showed remarkable antibacterial activities against *E. coli* compared to ciprofloxacin with MICs of 0.64 $\mu\text{g/mL}$, 0.18 $\mu\text{g/mL}$, 0.34 $\mu\text{g/mL}$, 0.53 $\mu\text{g/mL}$, and 0.15 $\mu\text{g/mL}$, respectively. Moreover, hybrids **2a**, **2b**, **2c** and **2e** showed moderate activity against *P. aeruginosa* compared to ciprofloxacin with MICs of 1.12 $\mu\text{g/mL}$, 0.64 $\mu\text{g/mL}$, 1.03 $\mu\text{g/mL}$, 0.96 $\mu\text{g/mL}$, and 0.22 $\mu\text{g/mL}$, respectively.

Concerning the antibacterial activities of hybrids **5a–i**, ciprofloxacin derivatives **5a**, **5b**, **5c**, **5e**, **5g**, **5h**, and **5i** exhibited potent antibacterial activities against *S. aureus* compared to ciprofloxacin with MICs of 0.36 $\mu\text{g/mL}$, 0.7 $\mu\text{g/mL}$, 0.58 $\mu\text{g/mL}$, 0.78 $\mu\text{g/mL}$, 0.28 $\mu\text{g/mL}$, 0.34 $\mu\text{g/mL}$, 0.74 $\mu\text{g/mL}$, and 3.25 $\mu\text{g/mL}$, respectively. Furthermore, hybrids **5a**, **5b**, **5e**, **5h**, and **5i** revealed moderate activities against *E. coli* compared to ciprofloxacin with MICs of 0.91 $\mu\text{g/mL}$, 0.12 $\mu\text{g/mL}$, 0.52 $\mu\text{g/mL}$, 0.21 $\mu\text{g/mL}$, 0.63 $\mu\text{g/mL}$, and 0.15 $\mu\text{g/mL}$, respectively, while pyrimidine

Table 1 In vitro antibacterial and antifungal activities of ciprofloxacin derivatives **2a-j**, **5a-i**, ciprofloxacin and ketoconazole

Compound	MIC ($\mu\text{g/mL}$)			
	Gram-positive		Gram-negative	
	<i>S. aureus</i>	<i>E. coli</i>	<i>P. aeruginosa</i>	Fungi <i>C. albicans</i>
1	0.70	0.60	1.20	>100
2a	0.74	0.64	1.12	>100
2b	0.06	0.18	0.64	15.23
2c	0.67	0.34	1.03	3.89
2d	2.65	4.78	7.25	>100
2e	0.89	0.53	0.96	2.03
2f	0.94	9.33	3.7	>100
2g	8	16.98	6.25	>100
2h	1.2	5.25	3.125	84.21
2i	6.3	4.13	17	>100
2j	1.48	5.13	4.2	>100
5a	0.36	0.91	1.53	6.23
5b	0.7	0.12	0.19	>100
5c	0.58	1.03	2.04	2.87
5d	8.14	42.23	12.30	36.12
5e	0.78	0.52	3.25	2.51
5f	4.79	3.89	2.95	>100
5g	0.28	14.25	23.12	>100
5h	0.34	0.21	0.49	28.73
5i	0.74	0.63	0.13	>100
Ciprofloxacin	3.25	0.15	0.22	>100
Ketoconazole	–	–	–	2.6

derivatives **5b** and **5i** showed potent antibacterial activities against *P. aeruginosa* compared to ciprofloxacin with MICs of 0.19 $\mu\text{g/mL}$, 0.13 $\mu\text{g/mL}$, and 0.22 $\mu\text{g/mL}$, respectively.

On the other hand, the antifungal results shown in Table 1, the antifungal activities of ciprofloxacin hybrids **2a-j**, only compound **2c** showed considerable antifungal activity against *C. albicans* compared to ketoconazole with MICs of 3.89 and 2.6 $\mu\text{g/mL}$, respectively. Moreover, pyrimidine derivatives **5e** displayed potent antifungal activity against *C. albicans* compared to ketoconazole with MICs of 2.51 and 2.60 $\mu\text{g/mL}$, respectively. Also, hybrids **5a** and **5c** exhibited considerable antifungal activities against *C. albicans* compared to ketoconazole with MICs of 6.23, 2.87, and 2.6 $\mu\text{g/mL}$, respectively.

Based on the antibacterial and antifungal results recorded in Table 1, it can be deduced that ciprofloxacin hybrids **2a-j** and **5a-i** showed higher antibacterial activity against Gram-positive bacteria (*S. aureus*) than Gram-negative bacteria (*E. coli* and *P. aeruginosa*). Compound **5b** displayed broad-spectrum antimicrobial activity against all tested strains except *C. albicans*. Concerning chalcone derivatives **2a-j**, it was found that the presence of electron-withdrawing group on the terminal phenyl ring of the chalcone moiety increases

the antibacterial activity and *meta* position was preferred. In term of potency, chlorine atom is superior to other halogens for monosubstituted derivatives. Shifting the chlorine atom from the *meta* position to the *para* position slightly decreased the antibacterial activity. Also, Replacement of chlorine atom at *para* position with fluorine enhanced the antibacterial activity. Furthermore, introduction of an electron-donating group on the terminal phenyl ring of the chalcone moiety markedly decreased the antibacterial activity. Additionally, regarding SAR studies of ciprofloxacin-pyrimidine hybrids **5a-i** as antibacterial agents, it was found that there is no specific substituent on the phenyl ring directly attached to the pyrimidine core of compounds **5a-j** could determine the activity either electron-donating or electron-withdrawing groups and the enhanced antibacterial activity of some of the pyrimidine derivatives may be attributed to the improvement of the physicochemical properties and consequently enhancing permeability to the bacterial cells. Regarding, SAR studies for antifungal activities of the newly synthesized ciprofloxacin derivatives **1**, **2a-j**, and **5a-i** revealed that the presence of electron-withdrawing group on the terminal phenyl ring of the chalcone moiety was found to improve the antifungal activity and *para* position is optimal for antifungal activity for monosubstituted derivatives. In term of potency, fluorine atom at *para* position was superior to other halogens. Furthermore, introduction of an electron-donating group on the terminal phenyl ring of the chalcone moiety or on the phenyl ring directly attached to the pyrimidine core was found to decrease or abolish the antifungal activity.

The Effect of ciprofloxacin hybrids on **2a-c**, **2e-f**, **5a-c**, **5e-i** and ciprofloxacin on *S. aureus* DNA gyrase catalytic activity

As antibacterial agents, fluoroquinolones act by targeting and inhibiting DNA gyrase (topo II) which is an essential enzyme involved in the DNA replication process [46–48]. During the processes of DNA replication, gyrase enzyme allows the relaxation of supercoiled DNA by breaking both strands of DNA chain, crossing them over, and then resealing them; hence, the DNA can unwind and replicate [49]. Based on the current design, the inhibitory activity of the most promising ciprofloxacin hybrids **2a-c**, **2e-f**, **5a-c**, and **5e-i** on DNA gyrase as potential molecular target was evaluated utilizing *S. aureus* DNA gyrase Elisa Kit and ciprofloxacin was used as reference. The results of DNA gyrase assay are outlined in Table 2. According to the results in Table 2, compounds **2b** showed potent inhibitory activity against DNA gyrase than the parent ciprofloxacin with IC_{50} of 0.231 μM and 0.323 μM , respectively. Other tested compounds showed good inhibitory activity against DNA gyrase compared to the reference ciprofloxacin with IC_{50} of 1.012–7.592 μM and 0.323 μM , respectively. Hence, it is

Table 2 The inhibitory activities of ciprofloxacin hybrids 2a-c, 2e-f, 5a-c, 5e-i and ciprofloxacin on *S. aureus* DNA gyrase

Compound	<i>S. aureus</i> DNA gyrase IC ₅₀ ± SD (μM)
2a	3.469 ± 0.18
2b	0.231 ± 0.01
2c	2.995 ± 0.16
2e	3.810 ± 0.20
2f	1.770 ± 0.09
5a	4.546 ± 0.24
5b	1.272 ± 0.07
5c	1.567 ± 0.08
5e	1.012 ± 0.05
5f	3.505 ± 0.19
5g	7.592 ± 0.40
5h	1.456 ± 0.08
5i	1.414 ± 0.07
Ciprofloxacin	0.323 ± 0.02

obvious that the enhanced antibacterial activity of the target ciprofloxacin derivatives could be attributed to inhibition of bacterial DNA gyrase.

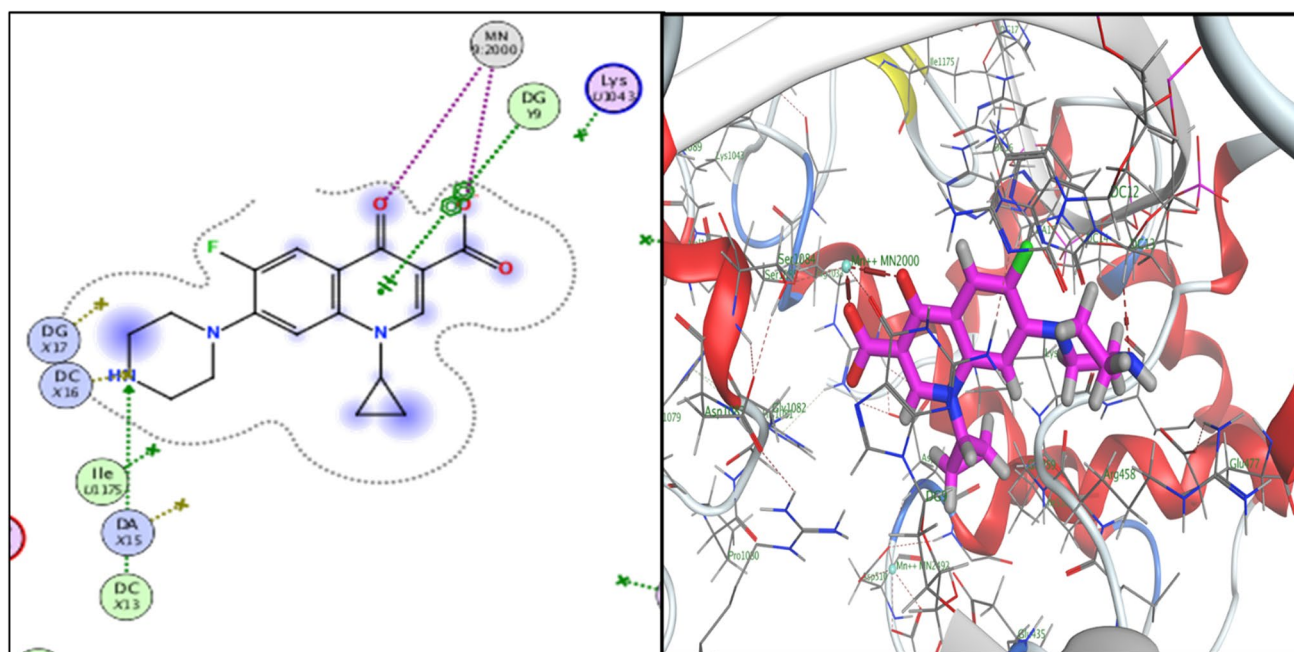
Docking studies on bacterial gyrase enzyme

Molecular docking investigation for the most active compounds **2b**, **2c**, **5a**, **5c**, **5e**, **5h**, and **5i** against *S. aureus*

was carried out using Molecular Operating Environment (MOE®) version 2014 to investigate their possible interactions within the active site of gyrase enzyme (PDB: 2XCT). The 3D crystal structure of gyrase enzyme was downloaded from PDB (ID: 2XCT) [50, 51]. Molecular modeling of the co-crystallized ligand (ciprofloxacin) revealed different types of interactions with the active site of gyrase enzyme including a chelation with Mn⁺² 9:2000, hydrogen bonding with DNA nucleotide base DC X13, hydrophobic interactions, and pi-cationic interaction with DNA nucleotide base DG Y9 (Figs. 2, 3). Also, docking studies of ciprofloxacin hybrids **2b**, **2c**, **5b**, **5c**, **5e**, **5h**, and **5i** revealed that they have the ability to interact with crystal structure of gyrase enzyme via hydrophobic interactions and extra hydrogen bonding interaction with amino acids residues and DNA nucleotide bases (Table 3, Figs. 4, 5, 6, 7 in Supplementary materials) which consistent with their enhanced antibacterial activity against *S. aureus*. All docked compounds had high binding affinity to gyrase enzyme as their energy scores (dG) values are (− 12.8884 to − 10.5550 kcal/mole) higher than that of the co-crystallized ligand ciprofloxacin (dG = − 8.7725 kcal/mole), Table 3. The binding-free energies and binding interactions from the major docked poses of ciprofloxacin hybrids **2b**, **2c**, **5a**, **5b**, **5c**, **5h**, and **5i** are listed in Table 3.

Determination of solubility and lipophilicity

Physicochemical properties of drug molecules are very important parameters that affect biological activity.

**Fig. 2** 2D- and 3D-binding interactions of ciprofloxacin within gyrase-active site (PDB:2XCT)

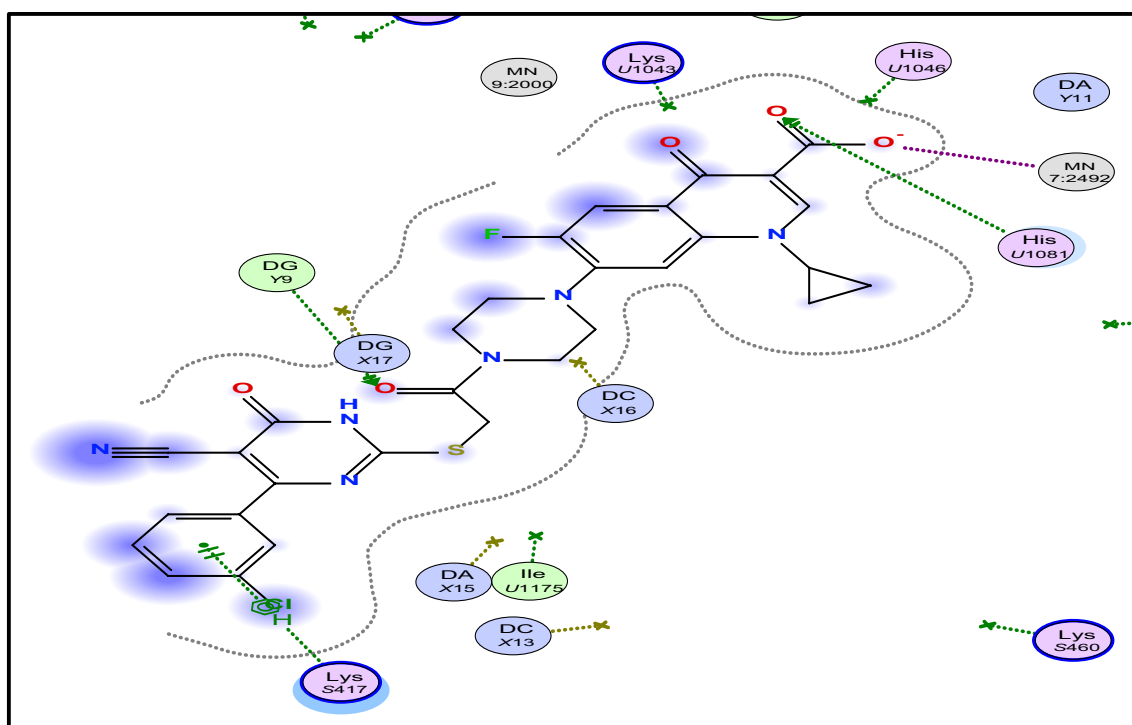


Fig. 3 2D-binding interactions of compound **2b** within gyrase-active site (PDB:2XCT)

Therefore, it is necessary to investigate the solubility and lipophilicity of some of the active series of the target compounds **2a-i**. The results of measuring solubility and lipophilicity are outlined in Table 4.

As shown in Table 4, the solubility studies of compounds **2a-i** in buffer solutions at pH 6.8 and 7.8 and temperature 37 ± 0.5 showed that the solubility values of the tested compounds are variable. The strength of the bond in ion solvates is expected to be more than that between the unionized forms of the molecules and solvent. Hence, solubility of the charged forms of the fluoroquinolone molecules is expected to exceed the solubility of a neutral analog [52]. The fluoroquinolones under study have a basic (N-) and acidic groups, (-COOH) and (-CONH). These polar groups in these molecules can participate in formation of hydrogen bonds with the solvent and strong intermolecular interactions.

Partition coefficient of ciprofloxacin hybrids **2a-j** between octanol and buffer solution was studied at temperature of 37 ± 0.5 and pH 7.8 using the isothermal saturation method. Results in Table 4 express the distribution coefficients of drugs in logarithmic scale obtained from the experimental concentrations in organic and water phases ($\log p$). [53, 54]. According to the distribution of fluoroquinolones in octanol/buffer pH 7.4 system, the lipophilicity of the tested compounds decreases in the following order: **2d** > **2f** > **2j** > **2b** > **2a**. Results from a similar study using enrofloxacin molecule [55] showed that a comparatively

high lipophilicity could be attributed to its less polar surface area. It is obvious that substitution at piperazinyl N-4 increased lipophilicity of the tested compounds that may be due to decrease in the possibility of zwitter ion formation. It is clear from Table 4 that the distribution coefficients decrease in buffer solutions at lower pH, the cationic species dominate in comparison with pH 7.4 when the zwitterionic forms predominate.

The observation that the fluoroquinolones which are secondary amines have increased partitioning at pH 5 as compared with the tertiary amines further suggests that ion pairing is a possible explanation because it has been observed that the order of ion-pair formation constants of amines is $3^\circ < 2^\circ < 1^\circ$ [56]. The order of ion-pairing has been attributed to the number of hydrogen atoms available to hydrogen bond with the anion and stabilized the ion pair.

Conclusion

New ciprofloxacin derivatives **2a-j** and **5a-i** were synthesized and investigated for their antibacterial activity. In general, ciprofloxacin hybrids **2a-j** and **5a-i** showed potent antibacterial activity against Gram-positive bacteria (*S. aureus*) than Gram-negative bacteria (*E. coli* and *P. aeruginosa*). On the other hand, compounds **2c**, **2e**, **5c**, and **5e** revealed comparable antifungal activity to

Table 3 Types of interactions and energy scores for interaction of ciprofloxacin derivatives **2b**, **2c**, **5a**, **5b**, **5c**, **5e**, **5h**, **5i**, and the reference ciprofloxacin within the active site of Bacterial gyrase (PDB: 2XCT)

#	Types of interactions	Energy score Kcal/mole
Ciprofloxacin	<ul style="list-style-type: none"> • Chelation with Mn⁺² 9:2000 via the C-3 carboxylic group and C-4 carbonyl functionality of quinolone moiety • Hydrogen bonding with DNA nucleotide base DC X13 • pi-cationic interaction with DNA nucleotide base DG Y9 • Hydrophobic interactions 	– 8.1332
2b	<ul style="list-style-type: none"> • Hydrogen bond with Mn⁺² 9:2492 via carbonyl of quinolone moiety • Hydrogen bond with His. 2084 via carbonyl of urea linker • Hydrogen bonding with DNA nucleotide base DG Y9 • pi-cationic interaction with Lys. S417 • Hydrophobic interactions 	– 10.0950
2c	<ul style="list-style-type: none"> • Hydrogen bond with Mn⁺² 9:2000 via carbonyl of quinolone moiety • Hydrogen bonding with DNA nucleotide base DG Y9 • Hydrophobic interactions 	– 9.5058
5a	<ul style="list-style-type: none"> • Hydrogen bond with Mn⁺² 7:2492 via carboxylic group of quinolone moiety • Hydrogen bond with His 1034 via carbonyl of carboxylic group • pi-cationic interaction with Arg. 158 Hydrophobic interactions 	– 10.0895
5b	<ul style="list-style-type: none"> • Hydrogen bond with Mn⁺² 7:2492 via carboxylic group of quinolone moiety • Hydrogen bond with His 1034 via carbonyl of carboxylic group • Hydrogen bonding with DNA nucleotide base DG Y9 • pi-cationic interaction with Lys. S117 • Hydrophobic interactions 	– 10.2850
5c	<ul style="list-style-type: none"> • Hydrogen bond with Mn⁺² 7:2492 via carboxylic group of quinolone moiety • Hydrogen bond with Glu. S477 and Arg. S158 • pi-cationic interaction with DNA nucleotide base DG Y9 Hydrophobic interactions 	– 9.9704
5e	<ul style="list-style-type: none"> • Chelation with Mn⁺² 9:2000 via the C-3 carboxylic group and C-4 carbonyl functionality of quinolone moiety • Hydrogen bonding with DNA nucleotide base DC X12 • Two pi-cationic interaction with DNA nucleotide base DG Y9 Hydrophobic interactions 	– 10.3587
5h	<ul style="list-style-type: none"> • Chelation with Mn⁺² 9:2000 via the C-3 carboxylic group and C-4 carbonyl functionality of quinolone moiety • Hydrogen bonding with Asn.S476 and Asn. S475 • Two pi-cationic interaction with DNA nucleotide base DG Y9 Hydrophobic interactions 	– 10.7105
5i	<ul style="list-style-type: none"> • Chelation with Mn⁺² 9:2000 via the C-3 carboxylic group and C-4 carbonyl functionality of quinolone moiety • Two pi-cationic interaction with DNA nucleotide base DG Y9 Hydrophobic interactions 	– 10.9547

ketoconazole against *candida albicans*. Further investigations showed that some ciprofloxacin hybrids have an inhibitory effect on the catalytic activity of DNA gyrase as potential molecular target. Structure activity relationship of hybrids **2a-j** indicated that the presence of electron-withdrawing group on the terminal phenyl ring of the chalcone moiety increases the antibacterial activity and meta position was preferred, while introduction of an electron-donating group markedly decreases the antibacterial activity. Regarding ciprofloxacin-pyrimidine hybrids **5a-i** as antibacterial agents, it was found that there is no specific substituent on the phenyl ring directly attached to the pyrimidine core of compounds **5a-j** could determine the activity either electron-donating or electron-withdrawing groups. Docking studies against DNA gyrase-active site

(PDB: 2XCT) confirmed the ability of compounds **2b**, **2c**, **5a**, **5b**, **5c**, and **5e** to interact with DNA gyrase enzyme.

Experimental

Chemistry

Materials and methods

All chemical and reagents used for synthetic procedures and biological evaluations were purchased from commercial suppliers. Chemical Reactions were monitored by analytical thin layer chromatography (TLC), using precoated silica gel 60 F245 aluminum plate. Melting points were recorded

Table 4 Solubility pHs of 6.8 and 7.8 at 37 °C (mg/mL) and lipophilicity expressed in (Log P_{exp}) of synthesized target compounds 2a-i and Ciprofloxacin

Compound #	Solubility mg/mL		Lipophilicity (log p)
	pH 6.8	pH 7.8	
Ciprofloxacin	0.12	0.16	− 0.56
2a	0.21	0.15	0.24
2b	0.16	0.18	0.31
2c	0.13	0.15	0.07
2d	0.14	0.16	0.42
2e	0.16	0.18	0.07
2f	0.16	0.17	0.4
5g	0.74	0.9	− 0.09
2j	0.18	0.15	0.34
2h	0.68	0.78	− 0.21
2i	0.15	0.19	− 0.06

on a Stuart SMP30 melting point apparatus and were uncorrected. NMR spectra (400 MHz for ^1H , 100 MHz for ^{13}C) were observed in DMSO- d_6 on Bruker AM400 spectrometer with tetramethylsilane as the internal standard. Elemental analyses were recorded on Shimadzu GC/MS-QP5050A, Regional center for Mycology and Biotechnology, Al-Azhar University, Cairo, Egypt. Mass spectra were recorded on Advion compact mass spectrometer (CMS) and reported as mass/charge (m/z), Nawah scientific center for research, Almokattam, Cairo, Egypt.

General procedure for synthesis of 7-(4-((4-cinamoylphenyl)carbamoyl)piperazin-1-yl)-1-cyclopropyl-6-fluoro-4-oxo-1,4-dihydroquinoline-3-carboxylic acid derivatives 2a-j

An equimolar amount of ciprofloxacin derivative 1 (0.492 g, 1 mmol) and the appropriate aromatic aldehyde (1.1 mmol) were dissolved in a minimum amount of ethanol, and aqueous NaOH (2.5 mmol) was added as 60% solution in a drop-wise manner. The reaction mixture was stirred in an ice bath for 30 min then at rt for 8–12 h then the reaction mixture was acidified with acetic acid. The formed precipitate was filtered off and washed thoroughly with cold-distilled water and cold methanol. The product was recrystallized from absolute ethanol [56].

General procedure for synthesis of 2-mercapto-6-oxo-4-phenyl-1,6-dihydropyrimidine-5-carbonitrile derivatives 3a-i

To a mixture of ethyl cyanoacetate (1.2 mL, 11.21 mmol), thiourea (0.85 g, 11.21 mmol) and the appropriate aldehyde (10.2 mmol) in 50 mL absolute ethanol, potassium carbonate

(1.56 g, 11.21 mmol) was added. The reaction mixture was heated under reflux for 6 h, cooled, poured into 50 mL distilled water, and acidified with few drops of glacial acetic acid to give a precipitate, which was filtered off, dried, and recrystallized from DMF/water to give compounds **8a-i** [40, 41]

General procedure for synthesis

of 7-(4-(2-((5-cyano-6-oxo-4-phenyl-1,6-dihydropyrimidin-2-yl)thio)acetyl)piperazin-1-yl)-1-cyclopropyl-6-fluoro-4-oxo-1,4-dihydroquinoline-3-carboxylic acid derivatives 5a-i

An equimolar mixture of compound **4** (0.30 g, 0.660 mmol) and intermediates **3a-i** (0.73 mmol) in acetonitrile (50 mL), and TEA (0.79 mmol, 0.20 mL) were added. The reaction mixture was heated at reflux for 6–8 h. The reaction mixture was evaporated to dryness. The residue was crystallized from acetonitrile to afford the target compounds **5a-i** [17].

7-(4-(2-((5-Cyano-6-oxo-4-phenyl-1,6-dihydropyrimidin-2-yl)thio)acetyl)piperazin-1-yl)-1-cyclopropyl-6-fluoro-4-oxo-1,4-dihydroquinoline-3-carboxylic acid 5a White powder; (0.29 g, 73.12% yield); mp: 237–240 °C; ^1H NMR (400 MHz, DMSO- d_6) δ : 1.18–1.22 (2H, m, cyclopropyl-*H*), 1.32–1.33 (2H, m, cyclopropyl-*H*), 3.30–3.38 (4H, m, piperazinyl-*H*), 3.71–3.78 (5H, m, piperazinyl-*H* and cyclopropyl-*H*), 4.42 (2H, s, S- CH_2), 7.53–7.58 (4H, m, Ar-*H* and C8-*H*), 7.93–7.96 (3H, m, Ar-*H* and C5-*H*), 8.68 (1H, s, C2-*H*), 14.29–14.35 (1H, brs, CO-NH), 15.15 (1H, brs, COOH); ^{13}C NMR (100 MHz, DMSO- d_6) δ : 8.07, 34.59, 38.81, 45.46, 49.49, 49.93, 93.43, 106.93, 107.34, 111.37, 111.58 (C-5, d, $^2J_{\text{FCortho}}=23$ Hz, C-F), 116.27, 119.32, 121.22, 123.96, 128.99, 132.17, 135.76, 136.87, 139.65, 145.25, 148.56, 153.37 (C-6, d, $^1J_{\text{FCipso}}=250$ Hz, C-F), 165.57, 166.33, 174.92; ESI-MS (m/z): Calcd. 600.16, found 599.70 [M-H] $^-$ Anal. Calcd. For $\text{C}_{30}\text{H}_{25}\text{FN}_6\text{O}_5\text{S}$: C, 59.99; H, 4.20; N, 13.99; S, 5.34. Found: C, 60.21; H, 4.37; N, 13.85; S, 5.41.

7-(4-(2-((4-(3-Chlorophenyl)-5-cyano-6-oxo-1,6-dihydropyrimidin-2-yl)thio)acetyl)piperazin-1-yl)-1-cyclopropyl-6-fluoro-4-oxo-1,4-dihydroquinoline-3-carboxylic acid 5b Yellow powder; (0.32 g, 76.23% yield); mp: 248–251 °C; ^1H NMR (400 MHz, DMSO- d_6) δ : 1.20–1.26 (2H, m, cyclopropyl-*H*), 1.32–1.33 (2H, m, cyclopropyl-*H*), 3.30–3.38 (4H, m, piperazinyl-*H*), 3.72–3.81 (5H, m, piperazinyl-*H* and cyclopropyl-*H*), 4.37 (2H, s, S- CH_2), 7.53 (1H, d, $J_{\text{HFmeta}}=8$ Hz, C8-*H*), 7.55–7.59 (2H, m, Ar-*H*), 7.87–7.89 (2H, m, Ar-*H*), 7.92 (1H, d, $J_{\text{HFortho}}=12$ Hz, C5-*H*), 8.68 (1H, s, C2-*H*), 11.98 (1H, brs, CO-NH), 15.15 (1H, brs, COOH); ^{13}C NMR (100 MHz, DMSO- d_6) δ : 8.07, 34.23, 36.34, 45.55, 49.46, 49.97, 93.35, 106.92, 107.34, 111.54

(C-5, d, $^2J_{\text{FCortho}}=23$ Hz, C-F), 112.66, 116.60, 127.71, 128.71, 130.86, 131.59, 131.76, 133.75, 138.09, 138.97, 139.64, 145.15, 148.54, 153.41 (C-6, d, $^1J_{\text{FCipso}}=245$ Hz, C-F), 165.84, 166.00, 166.34, 176.86; ESI-MS (m/z): Calcd. 634.12, found 633.07 [M-H]⁻. Anal. Calcd. For C₃₀H₂₄ClFN₆O₅S: C, 56.74; H, 3.81; N, 13.23; S, 5.05. Found: C, 56.86; H, 3.94; N, 13.49; S, 5.12.

7-(4-(2-((4-(4-Chlorophenyl)-5-cyano-6-oxo-1,6-dihydropyrimidin-2-yl)thio)acetyl)piperazin-1-yl)-1-cyclopropyl-6-fluoro-4-oxo-1,4-dihydroquinoline-3-carboxylic acid 5c Yellowish white powder; (0.31 g, 73.98% yield); mp: 253–256 °C; ¹H NMR (400 MHz, DMSO-*d*₆) δ: 1.20–1.22 (2H, m, cyclopropyl-*H*), 1.32–1.36 (2H, m, cyclopropyl-*H*), 3.34–3.39 (4H, m, piperazinyl-*H*), 3.72–3.85 (5H, m, piperazinyl-*H* and cyclopropyl-*H*), 4.22 (2H, s, S-CH₂), 7.55 (2H, d, *J* = 8 Hz, Ar-*H*), 7.58 (1H, d, $J_{\text{HFmeta}}=8$ Hz, C8-*H*), 7.87 (2H, d, *J* = 8 Hz, Ar-*H*), 7.93 (1H, d, $J_{\text{HFortho}}=13$ Hz, C5-*H*), 8.68 (1H, s, C2-*H*), 15.10 (1H, brs, COOH); ¹³C NMR (100 MHz, DMSO-*d*₆) δ: 8.02, 33.32, 36.32, 45.62, 49.14, 52.70, 91.27, 107.20, 111.75 (C-5, d, $^2J_{\text{FCortho}}=22$ Hz, C-F), 114.93, 120.26, 125.25, 126.28, 130.87, 131.71, 133.10, 137.75, 139.93, 142.07, 145.69, 150.52, 153.67 (C-6, d, $^1J_{\text{FCipso}}=2456$ Hz, C-F), 162.02, 164.55, 166.46, 176.38; ESI-MS (m/z): Calcd. 634.12, found 633.90 [M-H]⁻. Anal. Calcd. For C₃₀H₂₄ClFN₆O₅S: C, 56.74; H, 3.81; N, 13.23; S, 5.05. Found: C, 57.02; H, 3.94; N, 13.51; S, 5.21.

7-(4-(2-((4-(4-Bromophenyl)-5-cyano-6-oxo-1,6-dihydropyrimidin-2-yl)thio)acetyl)piperazin-1-yl)-1-cyclopropyl-6-fluoro-4-oxo-1,4-dihydroquinoline-3-carboxylic acid 5d Yellow powder; (0.35 g, 77.89% yield); mp: 284–285 °C; ¹H NMR (400 MHz, DMSO-*d*₆) δ: 1.20–1.27 (2H, m, cyclopropyl-*H*), 1.33–1.35 (2H, m, cyclopropyl-*H*), 3.36–3.41 (4H, m, piperazinyl-*H*), 3.71–3.83 (5H, m, piperazinyl-*H* and cyclopropyl-*H*), 4.40 (2H, s, S-CH₂), 7.53 (1H, d, $J_{\text{HFmeta}}=8$ Hz, C8-*H*), 7.73 (2H, d, *J* = 8 Hz, Ar-*H*), 7.86 (2H, d, *J* = 8 Hz, Ar-*H*), 7.93 (1H, d, $J_{\text{HFortho}}=16$ Hz, C5-*H*), 8.68 (1H, s, C2-*H*), 15.14 (1H, brs, COOH); ¹³C NMR (100 MHz, DMSO-*d*₆) δ: 8.06, 34.40, 36.33, 38.21, 44.04, 45.48, 49.36, 91.64, 107.35, 111.58 (C-5, d, $^2J_{\text{FCortho}}=23$ Hz, C-F), 114.41, 119.32, 121.23, 125.35, 131.18, 137.56, 139.21, 139.64, 145.28, 148.55, 151.15, 153.51 (C-6, d, $^1J_{\text{FCipso}}=245$ Hz, C-F), 158.64, 162.54, 165.44, 166.33, 177.06; ESI-MS (m/z): Calcd. 678.07, found 677.60 [M-H]⁻. Anal. Calcd. For C₃₀H₂₄BrFN₆O₅S: C, 53.03; H, 3.56; N, 12.37; S, 4.72. Found: C, 53.29; H, 3.52; N, 12.09; S, 4.81.

7-(4-(2-((4-(4-Fluorophenyl)-5-cyano-6-oxo-1,6-dihydropyrimidin-2-yl)thio)acetyl)piperazin-1-yl)-1-cyclopropyl-6-fluoro-4-oxo-1,4-dihydroquinoline-3-carboxylic acid 5e Pale yellow powder; (0.30 g, 73.11% yield); mp: 242–245 °C; ¹H NMR (400 MHz, DMSO-*d*₆) δ: 1.19–1.21

(2H, m, cyclopropyl-*H*), 1.32–1.33 (2H, m, cyclopropyl-*H*), 3.35–3.42 (4H, m, piperazinyl-*H*), 3.70–3.84 (5H, m, piperazinyl-*H* and cyclopropyl-*H*), 4.44 (2H, s, S-CH₂), 7.38 (2H, t, $J_{\text{HFortho}}=8$ Hz, Ar-*H*), 7.52 (1H, d, *J* = 8 Hz, C8-*H*), 7.92 (1H, d, $J_{\text{HFortho}}=12$ Hz, C5-*H*) 8.02 (2H, t, $J_{\text{F}}=8$ Hz, Ar-*H*), 8.67 (1H, s, C2-*H*), 15.14 (1H, brs, COOH); ¹³C NMR (100 MHz, DMSO-*d*₆) δ: 8.05, 34.74, 36.34, 44.72, 45.51, 49.62, 97.07, 107.01, 107.33, 111.53 (C-5, d, $^2J_{\text{FCortho}}=23$ Hz, C-F), 115.68 (C_{Ar}, d, $^2J_{\text{FCortho}}=21$ Hz, C-F), 119.39, 131.30, 133.50, 138.96, 139.65, 145.81, 146.64, 148.46, 148.63, 153.42 (C-6, d, $^1J_{\text{FCipso}}=245$ Hz, C-F), 155.21, 162.56 (C_{Ar}, d, $^1J_{\text{CFipso}}=286$ Hz, C-F), 165.00, 166.34, 176.86; ESI-MS (m/z): Calcd. 618.15, found 617.70 [M-H]⁻. Anal. Calcd. For C₃₀H₂₄F₂N₆O₅S: C, 58.25; H, 3.91; N, 13.59; S, 5.18. Found: C, 58.43; H, 4.12; N, 13.75; S, 5.34.

7-(4-(2-((5-Cyano-6-oxo-4-(*p*-tolyl)-1,6-dihydropyrimidin-2-yl)thio)acetyl)piperazin-1-yl)-1-cyclopropyl-6-fluoro-4-oxo-1,4-dihydroquinoline-3-carboxylic acid 10f-methyl 5f Pale yellow powder; (0.33 g, 80.95% yield); mp: 264–267 °C; ¹H NMR (400 MHz, DMSO-*d*₆) δ: 1.20–1.26 (2H, m, cyclopropyl-*H*), 1.33–1.34 (2H, m, cyclopropyl-*H*), 2.30 (3H, s, CH₃) 3.31–3.37 (4H, m, piperazinyl-*H*), 3.72–3.81 (5H, m, piperazinyl-*H* and cyclopropyl-*H*), 4.36 (2H, s, S-CH₂), 7.31 (2H, d, *J* = 8 Hz, Ar-*H*), 7.55 (1H, d, $J_{\text{HFmeta}}=8$ Hz, C8-*H*), 7.82 (2H, d, *J* = 8 Hz, Ar-*H*), 7.92 (1H, d, $J_{\text{HFortho}}=12$ Hz, C5-*H*), 8.67 (1H, s, C2-*H*), 13.62 (1H, brs, CO-NH), 15.13 (1H, brs, COOH); ¹³C NMR (100 MHz, DMSO-*d*₆) δ: 8.06, 20.80, 34.50, 36.33, 44.05, 49.67, 50.45, 92.77, 107.34, 108.72, 111.55 (C-5, d, $^2J_{\text{FCortho}}=23$ Hz, C-F), 112.29, 119.10, 123.40, 128.30, 131.18, 134.44, 138.04, 138.99, 140.20, 146.31, 148.54, 153.40 (C-6, d, $^1J_{\text{FCipso}}=242$ Hz, C-F), 161.74, 165.73, 166.31, 176.81; ESI-MS (m/z): Calcd. 614.18, found 613.80 [M-H]⁻. Anal. Calcd. For C₃₁H₂₇FN₆O₅S: C, 60.58; H, 4.43; N, 13.67; S, 5.22. Found: C, 60.31; H, 4.70; N, 13.90; S, 5.37.

7-(4-(2-((5-Cyano-4-(4-methoxyphenyl)-6-oxo-1,6-dihydropyrimidin-2-yl)thio)acetyl)piperazin-1-yl)-1-cyclopropyl-6-fluoro-4-oxo-1,4-dihydroquinoline-3-carboxylic acid 5g Pale yellow powder; (0.28 g, 67.15% yield); mp: 239–242 °C; ¹H NMR (400 MHz, DMSO-*d*₆) δ: 1.20–1.22 (2H, m, cyclopropyl-*H*), 1.31–1.33 (2H, m, cyclopropyl-*H*), 3.35–3.40 (4H, m, piperazinyl-*H*) 3.71–3.76 (4H, m, piperazinyl-*H*), 3.78–3.83 (4H, m, cyclopropyl-*H* and O-CH₃), 4.42 (2H, s, S-CH₂), 7.52–7.57 (3H, m, C8-*H* and Ar-*H*), 7.92–7.95 (3H, m, C5-*H* and Ar-*H*), 8.68 (1H, s, C2-*H*), 13.75 (1H, brs, CO-NH), 15.15 (1H, brs, COOH); ¹³C NMR (100 MHz, DMSO-*d*₆) δ: 8.01, 35.37, 36.28, 44.50, 49.83, 52.36, 55.36, 92.76 106.87, 107.20, 111.52 (C-5, d, $^2J_{\text{FCortho}}=23$ Hz, C-F), 120.19, 122.26, 126.45, 129.43, 130.94, 131.29, 135.06, 137.43, 139.65, 145.02, 148.46, 149.92, 153.39 (C-6, d,

$^1J_{\text{FCipso}}=246$ Hz, C-F), 165.98, 166.55, 175.76; ESI-MS (m/z): Calcd. 630.17, found 629.60 [M-H]⁻. Anal. Calcd. For C₃₁H₂₇FN₆O₆S: C, 59.04; H, 4.32; N, 13.33; S, 5.08. Found: C, 59.31; H, 4.50; N, 13.54; S, 5.17.

7-(4-(2-((5-Cyano-4-(3,4-dimethoxyphenyl)-6-oxo-1,6-dihydropyrimidin-2-yl)thio)acetyl)piperazin-1-yl)-1-cyclopropyl-6-fluoro-4-oxo-1,4-dihydroquinoline-3-carboxylic acid 5h. Pale yellow powder; (0.25g, 57.00% yield); mp: 266–269 °C; ^1H NMR (400 MHz, DMSO-*d*₆) δ : 1.17–1.21 (2H, m, cyclopropyl-*H*), 1.30–1.33 (2H, m, cyclopropyl-*H*), 3.29–3.37 (4H, m, piperazinyl-*H*), 3.71–3.76 (7H, m, piperazinyl-*H* and O-CH₃), 3.80–3.85 (4H, m, cyclopropyl-*H* and O-CH₃), 4.47 (2H, s, S-CH₂), 7.08 (1H, d, *J*=8 Hz, Ar-*H*), 7.53 (1H, d, $J_{\text{HFmeta}}=8$ Hz, C8-*H*), 7.64–7.67 (2H, m, Ar-*H*), 7.93 (1H, d, $J_{\text{HFortho}}=16$ Hz, C5-*H*), 8.68 (1H, s, C2-*H*), 13.92 (1H, brs, CO-NH), 15.14 (1H, brs, COOH); ^{13}C NMR (100 MHz, DMSO-*d*₆) δ : 8.05, 34.66, 36.30, 41.93, 45.53, 49.45, 56.21, 57.29, 91.77, 107.34, 111.55 (C-5, d, $^2J_{\text{FCortho}}=23$ Hz, C-F), 111.81, 112.93, 117.01, 119.37, 123.10, 127.86, 129.53, 132.41, 139.62, 145.16, 145.25, 148.52, 148.82, 152.12, 153.17 (C-6, d, $^1J_{\text{FCipso}}=246$ Hz, C-F), 161.36, 165.77, 166.35, 176.85; ESI-MS (m/z): Calcd. 660.18, found 659.60 [M-H]⁻. Anal. Calcd. For C₃₂H₂₉FN₆O₇S: C, 58.17; H, 4.42; N, 12.72; S, 4.85. Found: C, 58.29; H, 4.31; N, 12.95; S, 4.72.

7-(4-(2-((5-Cyano-6-oxo-4-(3,4,5-trimethoxyphenyl)-1,6-dihydropyrimidin-2-yl)thio)acetyl)piperazin-1-yl)-1-cyclopropyl-6-fluoro-4-oxo-1,4-dihydroquinoline-3-carboxylic acid 5i. Pale yellow powder; (0.23 g, 50. % yield); mp: 284–285 °C; ^1H NMR (400 MHz, DMSO-*d*₆) δ : 1.20–1.27 (2H, m, cyclopropyl-*H*), 1.32–1.34 (2H, m, cyclopropyl-*H*), 3.30–3.38 (4H, m, piperazinyl-*H*), 3.72 (3H, s, OCH₃), 3.74–3.83 (5H, m, piperazinyl-*H* and cyclopropyl-*H*), 3.86 (6H, s, OCH₃), 4.52 (2H, s, S-CH₂), 7.36 (2H, s, Ar-*H*), 7.53 (1H, d, $J_{\text{HFmeta}}=8$ Hz, C8-*H*) 7.92 (1H, d, $J_{\text{HFortho}}=12$ Hz, C5-*H*), 8.68 (1H, s, C2-*H*), 11.77 (1H, brs, CO-NH), 15.14 (1H, brs, COOH); ^{13}C NMR (100 MHz, DMSO-*d*₆) δ : 8.06, 34.98, 36.29, 41.89, 45.53, 49.44, 49.78, 56.70, 60.67, 92.81, 106.89, 107.47, 111.51 (C-5, d, $^2J_{\text{FCortho}}=23$ Hz, C-F), 116.61, 119.30, 126.54, 130.48, 134.78, 137.09, 139.58, 141.28, 145.14, 148.47, 152.09, 153.82 (C-6, d, $^1J_{\text{FCipso}}=257$ Hz, C-F), 161.74, 165.73, 166.31, 176.81; ESI-MS (m/z): Calcd. 690.19, found 689.60 [M-H]⁻. Anal. Calcd. For C₃₃H₃₁FN₆O₈S: C, 57.38; H, 4.52; N, 12.17; S, 4.64. Found: C, 57.56; H, 4.68; N, 12.34; S, 4.80.

Biology

Screening of the antimicrobial activity

Screening of the antibacterial activity. The antibacterial activity of compounds **1**, **2a-j**, and **5a-i** and ciprofloxacin

were determined according to the standard agar cup diffusion method [45] at Deraya University, Faculty of Pharmacy, Department of Microbiology and Faculty of Postgraduate Studies for Advanced Sciences, Beni-Suef University, Beni-Suef, Egypt.

Microbial strains and culture conditions Three bacterial species representing both Gram-positive and Gram-negative strains and were used to test the antibacterial activity of the newly synthesized ciprofloxacin derivatives. Standard strains of *Staphylococcus aureus* (ATCC 6538), *Pseudomonas aeruginosa* (ATCC 10,145), and *Escherichia coli* (ATCC 8739) were obtained from microbiological resource center, Faculty of Agriculture, Ain Shams University, Cairo, Egypt. All isolates were maintained at -70 °C in Trypticase Soya Broth (TSB, Becton, and Dickinson) with 10% glycerol. Prior to inoculation, all isolates were subcultured at 37 °C for 24 h on Trypticase Soya Agar (TSA, Becton, and Dickinson) and TSB, respectively.

Determination of the minimum inhibitory concentration (MIC) From all the tested bacteria 0.5 mL of 1×10^8 CFU/mL (0.5 McFarland turbidity) were plated in sterile petri dishes, then 20 mL of Mueller Hinton Agar media (Oxoid) was added to each petri dish. The plates were rotated slowly to ensure uniform distribution of the microorganisms and then allowed to solidify on a flat surface. After solidification, four equidistant and circular wells of 10 mm diameter were carefully punched using a sterile cork bore. Twofold serial dilutions of the tested compounds using DMSO were performed. An equal volume of 100 μ L of each dilution was applied separately to each well in three replicates using a micropipette. All plates were incubated at 37 °C for 24 h. The inhibition zones were measured, and their average was calculated. The MIC was calculated by plotting the natural logarithm of the concentration of each dilution of the tested compounds against the square of zones of inhibition, and a regression line was drawn through the points then the antilogarithm of the intercept on the logarithm of concentration axis gave the MIC value [57].

Screening of antifungal activity. The antifungal activity of compounds **1**, **2a-j**, and **5a-i** and ketoconazole were determined according to the agar cup diffusion method [45, 58] at Deraya University, Faculty of Pharmacy, Department of Microbiology.

Fungal strains and culture conditions. *Candida albicans* was used for screening of the antifungal activity of the newly synthesized ciprofloxacin derivatives. Standard strain of *Candida albicans* (ATCC 10,231) was obtained from microbiological resource center, Faculty of Agriculture, Ain Shams University, Cairo, Egypt. The isolate was maintained at -70 °C in Trypticase Soya Broth (TSB, Becton, and Dickinson) with 10% glycerol. Prior to

inoculation, the isolate was subcultured at 37°C for 24 h on Trypticase Soya Agar (TSA, Becton, and Dickinson) and TSB, respectively.

Determination of the minimum inhibitory concentration (MIC) From the tested *Candida albicans*, 0.5 mL of 1×10^8 CFU/mL (0.5 McFarland turbidity) was plated in sterile petri dishes, then 20 mL of Sabouraud agar was added to each petri dish. The plates were rotated slowly to ensure uniform distribution of the microorganisms and then allowed to solidify on a flat surface. After solidification, four equidistant and circular wells of 10 mm diameter were carefully punched using a sterile cork bore. Twofold serial dilutions of the tested compounds using DMSO were performed. An equal volume of 100 μ L of each dilution was applied separately to each well in three replicates using a micropipette. All plates were incubated at 37 °C for 24 h. The inhibition zones were measured, and their average was calculated. The MIC was calculated by plotting the natural logarithm of the concentration of each dilution of the tested compounds against the square of zones of inhibition and a regression line was drawn through the points then the antilogarithm of the intercept on the logarithm of concentration axis gave the MIC value [45, 58].

Staphylococcus aureus DNA Gyrase Supercoiling Assay *Staphylococcus aureus* DNA gyrase assay was performed according to established protocols obtained from inspirals (Cat. No. SAS4001) The new compounds and ciprofloxacin were dissolved in DMSO and serially diluted at concentrations of 100, 10, 1, and 0.1 μ M, and then assayed in reaction mixtures in three different replicate runs.

Staphylococcus aureus DNA gyrase was incubated at 37 °C for 30 min in a total reaction volume of 30 μ L containing 40 mM HEPES. KOH (pH 7.6), 10 mM magnesium acetate, 10 mM DTT, 2 mM ATP, 500 mM potassium glutamate, 0.05 mg/ml albumin and Relaxed pBR322. DNA gyrase supercoiling reactions catalyzed by *S. aureus* gyrase, Stop reaction by adding 30 μ L of STEB and 30 μ L of chloroform/isoamyl alcohol (v:v, 24:1), and then Vortex briefly ~ 5 secs and centrifuge for 1 min. after which 20 μ L of this was loaded on a 1% agarose gel that was then run at ~ 75 V for approximately 2 h. The gel was stained by (0.5 mg/L) ethidium bromide in water. Fluorescent images were taken at a wavelength of 300 nm on a UV transilluminator imaging system. The fluorescence intensity of the supercoiled plasmid reaction product was quantitated using ImaqQuant software (Molecular Dynamics). The results as IC50 values (concentration of the tested compound that leads to 50% inhibition of enzyme activity) for all samples were determined by nonlinear regression analysis in GraphPad Prism.

Docking studies on bacterial gyrase enzymes

All the compounds were drawn in Chem Draw professional (ver. 2015), converted to smiles, transferred to Molecular Operating Environment (MOE 2014) program. Hydrogens were added, and finally the energy of the docked structures was minimized using MMF94FX forcefield with a gradient RMS of 0.001 kcal/mol. Bacterial gyrase in complex with DNA and ciprofloxacin (2XCT) protein was downloaded from the RCSB Protein Data Bank (<https://www.rcsb.org/>). Bacterial gyrase in complex with DNA and ciprofloxacin X-ray crystal structure with 3.35 Å resolution (PDB ID: 2XCT) was used for docking studies. The protein was prepared by using the MOE quickprep protocol. The ligands were then docked in the binding site using the triangle matcher placement method. The number of generated poses was set for 10 for each ligand, and default settings were employed for other parameters. Refinement was carried out using Forcefield and scored using the affinity Δ G scoring system. To validate the docking study at the 2XCT-active site, the co-crystallized ligand was re-docked into the binding site using the same set of parameters as described above. The resulting docking poses were visually inspected, and the poses of the lowest binding-free energy value and with the best hydrophobic, H-bonding, and electrostatic interactions within the binding pocket of target protein.

Determination of solubility and lipophilicity

UV spectrophotometric scanning of drug

A sample of drug was accurately weighed and dissolved in 100 ml of distilled water to prepare 100 mcg/ml stock solutions. Appropriate dilution of the stock solution with phosphate buffer pH 6.8 and 7.8 was then made to prepare a working solution of 40mcg/ml. The absorbance of the drug in the working solution was scanned in the ultraviolet region (200–400 nm) to determine the wavelength of maximum absorbance ($\lambda_{\text{max}} = 272$ nm).

Construction of UV calibration curve

After determination of λ max of drug, a calibration curve was constructed by preparing solutions containing different concentrations of (1–5 mcg/ml) from stock solution after appropriate dilution with phosphate buffer pH 6.8. The UV absorbance of the prepared sample solutions were measured at the predetermined λ max using phosphate buffer pH 6.8 as a blank.

Solubility determinations

Aqueous solubility of the complexes was measured as a function of pH. An excess of each derivative was placed into suitable stoppered containers. Seven of these containers (in triplicate) were added with variable volumes of phosphate buffer to obtain pH values of 6.8 and 7.8. The samples were immersed in a water bath thermostated at $37 \pm 1^\circ\text{C}$ and 100 rpm and periodically shaken for 48 h. Once the equilibrium was reached, the pH of the supernatant was regarded. Aliquots of the filtrate properly diluted with suitable buffer were analyzed by UV spectrophotometry (Shimadzu *UV A-160*) at the maximum wavelengths (λ_{max} 272 nm) [57, 59].

Determination of partition coefficients

The n-octanol/water apparent partition coefficient at the isoelectric point (or distribution constant) was measured by using the traditional shake-flask technique. The pH of the aqueous buffer was first adjusted to isoelectric point of the compound. The n-octanol and aqueous phases were then mutually saturated before the measurement. The compound was dissolved in aqueous buffer solution and the solution was equilibrated with n-octanol for 1 h. The aqueous concentration to n-octanol concentration ratio ($C_{\text{aq}}/C_{\text{oct}}$) was 1:1. The samples were agitated for 5 h at water bath shaker thermostated at $25 \pm 1^\circ\text{C}$ and 100 rpm. The concentration of the solute was determined in the aqueous and organic phases at the isoelectric point by UV spectroscopy the log p value was calculated as follows:

$$\log p = \frac{[\text{conc. aq}]}{[\text{conc. oct}]}$$

Supplementary Information The online version contains supplementary material available at <https://doi.org/10.1007/s11030-022-10528-z>.

Author contributions The manuscript was written through contributions of all authors. All authors have given approval to the final version of the manuscript.

Funding Open access funding provided by The Science, Technology & Innovation Funding Authority (STDF) in cooperation with The Egyptian Knowledge Bank (EKB).

Declarations

Conflict of interest The authors declare that they have no known competing financial interests or personal relationships that could have appeared to influence the work reported in this manuscript. Authors declare that they do not have any conflict of interest. Authors declare that this manuscript is original, has not been published before, and is not currently being considered for publication elsewhere. We confirm that the manuscript has been read and approved by all named authors and that there are no other persons who satisfied the criteria for authorship

but are not listed. We further confirm that the order of authors listed in the manuscript has been approved by all of us.

Open Access This article is licensed under a Creative Commons Attribution 4.0 International License, which permits use, sharing, adaptation, distribution and reproduction in any medium or format, as long as you give appropriate credit to the original author(s) and the source, provide a link to the Creative Commons licence, and indicate if changes were made. The images or other third party material in this article are included in the article's Creative Commons licence, unless indicated otherwise in a credit line to the material. If material is not included in the article's Creative Commons licence and your intended use is not permitted by statutory regulation or exceeds the permitted use, you will need to obtain permission directly from the copyright holder. To view a copy of this licence, visit <http://creativecommons.org/licenses/by/4.0/>.

References


1. El-Etrawy A-AS, Sherbiny FF (2021) Design, synthesis, biological assessment and molecular docking studies of some new 2-Thioxo-2,3-dihydropyrimidin-4(1H)-ones as potential anticancer and antibacterial agents. *J Mol Struct* 1225:129014. <https://doi.org/10.1016/j.molstruc.2020.129014>
2. Liu H, Xia D-G, Chu Z-W et al (2020) Novel coumarin-thiazolyl ester derivatives as potential DNA gyrase Inhibitors: design, synthesis, and antibacterial activity. *Bioorg Chem* 100:103907. <https://doi.org/10.1016/j.bioorg.2020.103907>
3. Panda SS, Liaqat S, Girgis AS et al (2015) Novel antibacterial active quinolone-fluoroquinolone conjugates and 2D-QSAR studies. *Bioorg Med Chem Lett* 25:3816–3821. <https://doi.org/10.1016/j.bmcl.2015.07.077>
4. Payne DJ, Gwynn MN, Holmes DJ, Pompliano DL (2007) Drugs for bad bugs: confronting the challenges of antibacterial discovery. *Nat Rev Drug Discov* 6:29–40. <https://doi.org/10.1038/nrd2201>
5. Wenciewicz TA, Long TE, Möllmann U, Miller MJ (2013) Trihydroxamate siderophore-fluoroquinolone conjugates are selective sideromycin antibiotics that target *Staphylococcus aureus*. *Bioconj Chem* 24:473–486. <https://doi.org/10.1021/bc300610f>
6. Pokrovskaya V, Baasov T (2010) Dual-acting hybrid antibiotics: a promising strategy to combat bacterial resistance. *Expert Opin Drug Discov* 5:883–902. <https://doi.org/10.1517/17460441.2010.508069>
7. Domalaon R, Idowu T, Zhanel GG, Schweizer F (2018) Antibiotic hybrids: the next generation of agents and adjuvants against gram-negative pathogens? *Clin Microbiol Rev*. <https://doi.org/10.1128/CMR.00077-17>
8. Singh G, Arora A, Kalra P et al (2019) A strategic approach to the synthesis of ferrocene appended chalcone linked triazole allied organosilatrane: antibacterial, antifungal, antiparasitic and antioxidant studies. *Bioorg Med Chem* 27:188–195. <https://doi.org/10.1016/j.bmc.2018.11.038>
9. Fedorowicz J, Sączewski J (2018) Modifications of quinolones and fluoroquinolones: hybrid compounds and dual-action molecules. *Monatsh Chem* 149:1199–1245. <https://doi.org/10.1007/s00706-018-2215-x>
10. Mohammed HHH, Abuo-Rahma GE-DAA, Abbas SH, Abdelhafez E-SMN (2019) Current trends and future directions of fluoroquinolones. *Curr Med Chem* 26:3132–3149. <https://doi.org/10.2174/0929867325666180214122944>
11. Aziz HA, Moustafa GAI, Abuo-Rahma GE-DA et al (2020) Synthesis and antimicrobial evaluation of new nitric oxide-donating fluoroquinolone/oxime hybrids. *Arch Pharm*. <https://doi.org/10.1002/ardp.202000180>

12. Ezelarab HAA, Abbas SH, Hassan HA, Abuo-Rahma GE-DA (2018) Recent updates of fluoroquinolones as antibacterial agents. *Arch Pharm (Weinheim)* 351:e1800141. <https://doi.org/10.1002/ardp.201800141>
13. Mitscher LA, Ma Z (2003) Structure-activity relationships of quinolones. In: Ronald AR, Low DE (eds) *Fluoroquinolone antibiotics*. Birkhäuser, Basel, pp 11–48
14. Aldred KJ, Kerns RJ, Osheroff N (2014) Mechanism of quinolone action and resistance. *Biochemistry* 53:1565–1574. <https://doi.org/10.1021/bi5000564>
15. Mustaev A, Malik M, Zhao X et al (2014) Fluoroquinolone-gyrase-DNA complexes: two modes of drug binding. *J Biol Chem* 289:12300–12312. <https://doi.org/10.1074/jbc.M113.529164>
16. Mohammed HHH, Abdelhafez E-SMN, Abbas SH et al (2019) Design, synthesis and molecular docking of new N-4-piperazinyl ciprofloxacin-triazole hybrids with potential antimicrobial activity. *Bioorg Chem* 88:102952. <https://doi.org/10.1016/j.bioorg.2019.102952>
17. Mohammed HHH, Abbas SH, Abdelhafez E-SMN et al (2019) Synthesis, molecular docking, antimicrobial evaluation, and DNA cleavage assay of new thiadiazole/oxadiazole ciprofloxacin derivatives. *Monatsh Chem* 150:1809–1824. <https://doi.org/10.1007/s00706-019-02478-4>
18. Mermer A, Demirci S, Ozdemir SB et al (2017) Conventional and microwave irradiated synthesis, biological activity evaluation and molecular docking studies of highly substituted piperazine-azole hybrids. *Chin Chem Lett* 28:995–1005. <https://doi.org/10.1016/j.cclet.2016.12.012>
19. Ozdemir SB, Cebeci YU, Bayrak H et al (2017) Synthesis and antimicrobial activity of new piperazine-based heterocyclic compounds. *Heterocycl Commun* 23:43–54. <https://doi.org/10.1515/hc-2016-0125>
20. Gordeev MF, Hackbarth C, Barbachyn MR et al (2003) Novel oxazolidinone-quinolone hybrid antimicrobials. *Bioorg Med Chem Lett* 13:4213–4216. <https://doi.org/10.1016/j.bmcl.2003.07.021>
21. Dan W, Dai J (2020) Recent developments of chalcones as potential antibacterial agents in medicinal chemistry. *Eur J Med Chem* 187:111980. <https://doi.org/10.1016/j.ejmech.2019.111980>
22. da Silva PT, da Cunha XJ, Freitas TS et al (2021) Synthesis, spectroscopic characterization and antibacterial evaluation by chalcones derived of acetophenone isolated from *Croton anisodontus* Müll. *Arg Journal of Molecular Structure* 1226:129403. <https://doi.org/10.1016/j.molstruc.2020.129403>
23. Sashidhara KV, Rao KB, Kushwaha P et al (2015) Novel chalcone-thiazole hybrids as potent inhibitors of drug resistant *Staphylococcus aureus*. *ACS Med Chem Lett* 6:809–813. <https://doi.org/10.1021/acsmedchemlett.5b00169>
24. Khan SA, Asiri AM (2017) Green synthesis, characterization and biological evaluation of novel chalcones as anti bacterial agents. *Arab J Chem* 10:S2890–S2895. <https://doi.org/10.1016/j.arabjc.2013.11.018>
25. Insuasty B, Ramírez J, Becerra D et al (2015) An efficient synthesis of new caffeine-based chalcones, pyrazolines and pyrazolo[3,4-b][1,4]diazepines as potential antimalarial, antitrypanosomal and antileishmanial agents. *Eur J Med Chem* 93:401–413. <https://doi.org/10.1016/j.ejmech.2015.02.040>
26. Lahtchev KL, Batovska DI, Parushev SP et al (2008) Antifungal activity of chalcones: a mechanistic study using various yeast strains. *Eur J Med Chem* 43:2220–2228. <https://doi.org/10.1016/j.ejmech.2007.12.027>
27. Cheenpracha S, Karalai C, Ponglimanont C et al (2006) Anti-HIV-1 protease activity of compounds from *Boesenbergia pandurata*. *Bioorg Med Chem* 14:1710–1714. <https://doi.org/10.1016/j.bmc.2005.10.019>
28. Nowakowska Z (2007) A review of anti-infective and anti-inflammatory chalcones. *Eur J Med Chem* 42:125–137. <https://doi.org/10.1016/j.ejmech.2006.09.019>
29. Fathy M, Sun S, Zhao Q-L et al (2020) A new ciprofloxacin-derivative inhibits proliferation and suppresses the migration ability of HeLa cells. *Anticancer Res* 40:5025–5033. <https://doi.org/10.21873/anticancer.14505>
30. Mohammed HHH, Abbas SH, Hayallah AM et al (2020) Novel urea linked ciprofloxacin-chalcone hybrids having antiproliferative topoisomerases I/II inhibitory activities and caspases-mediated apoptosis. *Bioorg Chem*. <https://doi.org/10.1016/j.bioorg.2020.104422>
31. Suresh L, Poornachandra Y, Kanakaraju S et al (2015) One-pot three-component domino protocol for the synthesis of novel pyrano[2,3-d]pyrimidines as antimicrobial and anti-biofilm agents. *Org Biomol Chem* 13:7294–7306. <https://doi.org/10.1039/C5OB00693G>
32. Chate AV, Kamdi SP, Bhagat AN et al (2018) Design, synthesis and SAR study of novel spiro [pyrimido[5,4-b]quinoline-10,5'-pyrrolo[2,3-d]pyrimidine] derivatives as promising anticancer agents: design, synthesis and sar study of novel spiro [pyrimido[5,4-b]quinoline-10,5'-pyrrolo[2,3-d]pyrimidine] derivatives as promising anticancer agents. *J Heterocyclic Chem* 55:2297–2302. <https://doi.org/10.1002/jhet.3286>
33. Sharma V, Chitranshi N, Agarwal AK (2014) Significance and biological importance of pyrimidine in the microbial world. *Int J Med Chem* 2014:1–31. <https://doi.org/10.1155/2014/202784>
34. Ke S, Wei Y, Yang Z et al (2013) Novel cycloalkylthiophene-imine derivatives bearing benzothiazole scaffold: synthesis, characterization and antiviral activity evaluation. *Bioorg Med Chem Lett* 23:5131–5134. <https://doi.org/10.1016/j.bmcl.2013.07.023>
35. Padmavathi V, Sudhakar Reddy G, Padmaja A et al (2009) Synthesis, antimicrobial and cytotoxic activities of 1,3,4-oxadiazoles, 1,3,4-thiadiazoles and 1,2,4-triazoles. *Eur J Med Chem* 44:2106–2112. <https://doi.org/10.1016/j.ejmech.2008.10.012>
36. Dofe VS, Sarkate AP, Shaikh ZM et al (2018) Ultrasound-assisted synthesis of novel pyrazole and pyrimidine derivatives as antimicrobial agents: ultrasound-assisted synthesis of novel pyrazole and pyrimidine derivatives as antimicrobial agents. *J Heterocyclic Chem* 55:756–762. <https://doi.org/10.1002/jhet.3105>
37. Zha G-F, Leng J, Darshini N et al (2017) Synthesis, SAR and molecular docking studies of benzo[d]thiazole-hydrazones as potential antibacterial and antifungal agents. *Bioorg Med Chem Lett* 27:3148–3155. <https://doi.org/10.1016/j.bmcl.2017.05.032>
38. Akolkar SV, Nagargoje AA, Krishna VS et al (2019) New N-phenylacetamide-incorporated 1,2,3-triazoles: [Et₃NH][OAc]-mediated efficient synthesis and biological evaluation. *RSC Adv* 9:22080–22091. <https://doi.org/10.1039/C9RA03425K>
39. Shaquizzaman M, Khan SA, Amir M, Alam MM (2012) Synthesis, anticonvulsant and neurotoxicity evaluation of some new pyrimidine-5-carbonitrile derivatives. *Saudi Pharm J* 20:149. <https://doi.org/10.1016/j.jsps.2011.09.007>
40. Kaur H, Balzarini J, de Kock C et al (2015) Synthesis, antiplasmodial activity and mechanistic studies of pyrimidine-5-carbonitrile and quinoline hybrids. *Eur J Med Chem* 101:52–62. <https://doi.org/10.1016/j.ejmech.2015.06.024>
41. Zhou W, Ma L, Ding L et al (2019) Potent 5-cyano-6-phenylpyrimidin-based derivatives targeting DCN1–UBE2M interaction. *J Med Chem* 62:5382–5403. <https://doi.org/10.1021/acs.jmedchem.9b00003>
42. Aziz HA, El-Saghier AMM, Badr M et al (2021) Thiazolidine-2,4-dione-linked ciprofloxacin derivatives with broad-spectrum antibacterial MRSA and topoisomerase inhibitory activities. *Mol Divers*. <https://doi.org/10.1007/s11030-021-10302-7>

43. Smith JG (2010) Organic chemistry, 3rd edn. McGraw-Hill, New York
44. Solomons TWG, Fryhle CB (1998) Organic chemistry, 7th edn. Wiley, New York
45. Bonev B, Hooper J, Parisot J (2008) Principles of assessing bacterial susceptibility to antibiotics using the agar diffusion method. *J Antimicrob Chemother* 61:1295–1301. <https://doi.org/10.1093/jac/dkn090>
46. Redgrave LS, Sutton SB, Webber MA, Piddock LJV (2014) Fluoroquinolone resistance: mechanisms, impact on bacteria, and role in evolutionary success. *Trends Microbiol* 22:438–445. <https://doi.org/10.1016/j.tim.2014.04.007>
47. Hooper DC (1999) Mode of action of fluoroquinolones. *Drugs* 58(Suppl 2):6–10
48. Anderson VE, Osheroff N (2001) Type II topoisomerases as targets for quinolone antibacterials: turning Dr. Jekyll into Mr. Hyde. *Curr Pharm Des* 7:337–353
49. Champoux JJ (2001) DNA topoisomerases: structure, function, and mechanism. *Annu Rev Biochem* 70:369–413. <https://doi.org/10.1146/annurev.biochem.70.1.369>
50. Hassan AS, Askar AA, Nossier ES et al (2019) Antibacterial evaluation, in silico characters and molecular docking of Schiff bases derived from 5-aminopyrazoles. *Molecules* 24:3130. <https://doi.org/10.3390/molecules24173130>
51. Bax BD, Chan PF, Eggleston DS et al (2010) Type IIA topoisomerase inhibition by a new class of antibacterial agents. *Nature* 466:935–940. <https://doi.org/10.1038/nature09197>
52. Abdel-Aziz M, Park S-E, Abu-Rahma GE-DAA et al (2013) Novel N-4-piperazinyl-ciprofloxacin-chalcone hybrids: synthesis, physicochemical properties, anticancer and topoisomerase I and II inhibitory activity. *Eur J Med Chem* 69:427–438. <https://doi.org/10.1016/j.ejmech.2013.08.040>
53. Lambert A, Regnouf-de-Vains J, Ruiz-López M (2007). Structure of levofloxacin in hydrophilic and hydrophobic media: relationship to its antibacterial properties. <https://doi.org/10.1016/J.CPLETT.2007.05.077>
54. Kłosińska-Szmurło E, Grudzień M, Betlejewska-Kielak K et al (2014) Physicochemical properties of lomefloxacin, levofloxacin, and moxifloxacin relevant to the biopharmaceutics classification system. *Acta Chim Slov* 61:827–834
55. Bergström CAS, Strafford M, Lazorova L et al (2003) Absorption classification of oral drugs based on molecular surface properties. *J Med Chem* 46:558–570. <https://doi.org/10.1021/jm020986i>
56. Abou-Zied HA, Youssif BGM, Mohamed MFA et al (2019) EGFR inhibitors and apoptotic inducers: design, synthesis, anticancer activity and docking studies of novel xanthine derivatives carrying chalcone moiety as hybrid molecules. *Bioorg Chem* 89:102997. <https://doi.org/10.1016/j.bioorg.2019.102997>
57. Abdel-Aal AA, Abdel-Aziz SA, Shaykoon MSA et al (2019) Antibacterial and urease inhibitory activity of new piperazinyl n-4 functionalized ciprofloxacin-oxadiazoles. *J Mod Res* 1:1–7. <https://doi.org/10.21608/jmr.2019.12650.1001>
58. Ezelarab HAA, Hassan HA, Abbas SH et al (2018) Design, synthesis and antifungal activity of 1,2,4-triazole/or 1,3,4-oxadiazole-ciprofloxacin hybrids. *J Adv Biomed Pharm Sci* 1:78–84. <https://doi.org/10.21608/jabps.2018.3774.1013>
59. Ahadi H, Emami S (2020) Modification of 7-piperazinylquinolone antibacterials to promising anticancer lead compounds: synthesis and in vitro studies. *Eur J Med Chem* 187:111970. <https://doi.org/10.1016/j.ejmech.2019.111970>

Publisher's Note Springer Nature remains neutral with regard to jurisdictional claims in published maps and institutional affiliations.

Authors and Affiliations

Hamada H. H. Mohammed^{1,2,3}  · Doaa Mohamed Elroby Ali⁴ · Mohamed Badr⁵ · Ahmed G. K. Habib⁶ · Abobakr Mohamed Mahmoud⁷ · Sarah M. Farhan⁷ · Shimaa Salah Hassan Abd El Gany⁷ · Soad A. Mohamad⁸ · Alaa M. Hayallah^{9,10} · Samar H. Abbas² · Gamal El-Din A. Abu-Rahma^{2,3}

✉ Hamada H. H. Mohammed
hamada.hashem@pharm.sohag.edu.eg

✉ Gamal El-Din A. Abu-Rahma
gamal.aborahama@mu.edu.eg

¹ Department of Pharmaceutical Chemistry, Faculty of Pharmacy, Sohag University, Sohag 82524, Egypt

² Department of Medicinal Chemistry, Faculty of Pharmacy, Minia University, Minia 61519, Egypt

³ Department of Pharmaceutical Chemistry, Faculty of Pharmacy, Deraya University, New Minia City 61768, Egypt

⁴ Department of Biochemistry, Faculty of Pharmacy, Sohag University, Sohag 82524, Egypt

⁵ Department of Biochemistry, Faculty of Pharmacy, Menoufia University, Menoufia, Egypt

⁶ Department of Biotechnology and Life Sciences, Faculty of Postgraduate Studies for Advanced Sciences, Beni-Suef University, Beni-Suef, Egypt

⁷ Department of Microbiology and Immunology, Faculty of Pharmacy, Deraya University, New Minia City 61768, Egypt

⁸ Department of Pharmaceutics and Clinical Pharmacy, Faculty of Pharmacy, Deraya University, New Minia, Minya 61768, Egypt

⁹ Pharmaceutical Organic Chemistry Department, Faculty of Pharmacy, Assiut University, El Fateh 71526, Egypt

¹⁰ Pharmaceutical Chemistry Department, Faculty of Pharmacy, Sphinx University, New Assiut, Egypt